LEVEL II

AFGL-TR-78-0094

MONTE CARLO SIMULATION OF NEGATIVE ION COLLECTION BY A ROCKET-BORNE MASS SPECTROMETER

Takashi Sugimura

TRW Systems Group
One Space Park
Redondo Beach, California 90278

March 1978

Scientific Report No. 1

Approved for public release; distribution unlimited.

AIR FORCE GEOPHYSICS LABORATORY
AIR FORCE SYSTEMS COMMAND
UNITED STATES AIR FORCE
HANSCOM AFB, MASSACHUSETTS 01731

UNCLASSIFIED

SECURITY CLASSIFICATION OF THIS PAGE (When Data Entered)

REPORT DOCUMENTATION PAGE	READ INSTRUCTIONS BEFORE COMPLETING FORM
1. REPORT NUMBER (18) AFGL-TR-78-0094 (19)	2. GOVT ACCESSION NO.
3. RECIPIENT'S CATALOG NUMBER (9)	
4. TITLE (and Subtitle) (6) MONTE CARLO SIMULATION OF NEGATIVE ION COLLECTION BY A ROCKET-BORNE MASS SPECTROMETER	5. TYPE OF REPORT & PERIOD COVERED Scientific Interim rept.
	6. PERFORMING ORG. REPORT NUMBER Scientific Report No. 1
7. AUTHOR(s) (10) Takashi Sugimura	8. CONTRACT OR GRANT NUMBER(s) (15) F19628-77-C-0020 new
9. PERFORMING ORGANIZATION NAME AND ADDRESS TRW Systems Group, One Space Park, Redondo Beach, California 90278 (Beyond P space)	10. PROGRAM ELEMENT, PROJECT, TASK AREA & WORK UNIT NUMBERS (16) 61102F 2310G3AC (17) G3
11. CONTROLLING OFFICE NAME AND ADDRESS Air Force Geophysics Laboratory, Hanscom AFB, Mass. 91731, Contract Monitor: Dr. C. Sherman/LKD	12. REPORT DATE (11) March 1978
	13. NUMBER OF PAGES 28
14. MONITORING AGENCY NAME & ADDRESS (if different from Controlling Office) (12) 36p.	15. SECURITY CLASS. (of this report) unclassified
	15a. DECLASSIFICATION/DOWNGRADING SCHEDULE

16. DISTRIBUTION STATEMENT (of this Report)

Approved for public release; distribution unlimited.

17. DISTRIBUTION STATEMENT (of the abstract entered in Block 20, if different from Report)

(14) SCIENTIFIC-1

18. SUPPLEMENTARY NOTES

19. KEY WORDS (Continue on reverse side if necessary and identify by block number)

Monte Carlo
Ion flux
Free molecule flow
Transitional regime
Debye length
Plasma sheath
Rocket-borne probes

20. ABSTRACT (Continue on reverse side if necessary and identify by block number)

The Direct Simulation Monte Carlo Method developed for the prediction of positive ion collection by a rocket-borne probe has been extended to simulate negative ion effects. Major program modifications were necessary to properly describe the electron motion. In order to verify that the charged particle interactions were computed correctly a series of numerical experiments were → next page

DD FORM 1 JAN 73 1473 EDITION OF 1 NOV 65 IS OBSOLETE

UNCLASSIFIED

SECURITY CLASSIFICATION OF THIS PAGE (When Data Entered)

performed. The results of these calculations indicate that both the electron and ion mobilities are simulated properly in the presence of an applied electric field.

ACKNOWLEDGEMENT

The author thanks C. Sherman of AFGL and G. A. Bird from the University of Sydney, Australia for helpful suggestions concerning this study.

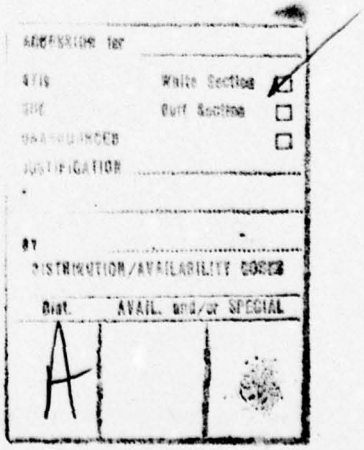

TABLE OF CONTENTS

NOMENCLATURE

A_D	collecting disc area
$C_I = \frac{N_i}{n_{i_\infty} u_\infty A_D}$	ion flux coefficient
D	diameter
E	electric field
e	charge on electron
K	mobility
k	Boltzmann's constant
m	mass
m*	reduced mass
N	number density
p	pressure
Q	collision cross section
$S = u_\infty \sqrt{\frac{2kT_\infty}{m}}$	speed ratio
T	temperature
U	velocity
$\overline{V} = \sqrt{\frac{2kT}{m}}$	thermal velocity
V_d	drift velocity
$\alpha =$	r_o/r_e
$\gamma =$	ϕ_o/ϕ_e
λ_∞	mean free path
λ_D	Debye length
μ	polarizability

σ	particle diameter
ϕ	electric potential

Subscripts

∞	free stream conditions
e	electron
i	ion

1. INTRODUCTION

A unique computational procedure to predict the flux of positive ions to a rocket-borne mass spectrometer has been developed under previous contracts. This procedure is the Direct Simulation Monte Carlo Method applied to charged particles. The method developed initially for neutral gases has been extended to a plasma in the presence of a charged body with a consistent electric field. Since the electric potential distribution required a solution of Poisson's equation, the charged particle calculations required an iteration procedure between the Monte Carlo results and a finite difference solution of Poisson's equation. The detailed formulation and results obtained for the collection of positive ions are given in references 1 through 4.

In the present study, the computer code developed for the positive ion collection has been modified to predict the flux of negative ions to a rocket-borne mass spectrometer. The major modification was the calculation of the electron trajectories which were ignored in the previous studies.

2. TECHNICAL APPROACH

2.1 PROBLEM FORMULATION FOR NEGATIVE ION ANALYSIS

In previous studies, e.g., references 1 through 3, the TRW Monte Carlo direct simulation has been used to predict the positive ion flux to a rocket borne mass spectrometer. A systematic variation of parameters was performed for the following variables: speed ratio, mean free path, Debye length, and applied collecting potential. The predictions and trends resulting from the parametric study will be helpful in understanding flight data and in the design of future instruments. Also included in the previous studies were the following effects: internal degrees of freedom, angle of attack, and space charge build-up on the vehicle sidewalls.

The assumptions and the complete formulation of the Monte Carlo simulation are detailed in Reference 1. Most important of the assumptions regards the treatment of the electrons. For the positive ion collection, the front face is negatively charged which repels the electrons and attracts the positive ions. The negative front face potential was assumed large enough so that the electrons could be taken to be in equilibrium with the local potential and determined by the Boltzmann distribution.

$$\frac{N_e}{N_{e\infty}} = e^{(e\phi/kT_e)} \tag{1}$$

where

N_e = electron number density

$N_{e\infty}$ = free stream value

ϕ = electric potential

T_e = electron temperature

e = charge on electron

This assumption was shown to be accurate in Reference 1 and was then used throughout the previous studies. The great simplification of this assumption was that the electron trajectories could be ignored and only the ion motion was computed with the only coupling between the ion and electron distributions occurring through the electric potential determined from Poisson's equation

$$\nabla^2\phi = \left(\frac{\lambda_\infty}{\lambda_D}\right)^2 (\bar{N}_i^+ - \bar{N}_e) \qquad (2)$$

where $\phi = \frac{e\phi}{kT_\infty}$ = non-dimensional electric potential

λ_∞ = mean free path

λ_D = Debye length

$\bar{N}_i^+ = \frac{N_i^+}{N_{i\infty}}$ = positive ion number density ratio

$\bar{N}_e = \frac{N_e}{N_{e\infty}}$ = electron number density ratio

In the present study, the negative ion flux to a rocket borne mass spectrometer is investigated. The collection of negative ions requires a positive collecting potential on the front face. This positive potential, however, also attracts the electrons which will reduce the collecting potential and the effectiveness of the instrument. The sampling of negative ions requires a circular double disk configuration; Reference 5, on the front face to repel the electrons while still collecting negative ions. The geometry and the potential distribution along the front face of the instrument payload will be approximated as shown in Figure 1. Although the face potential, Φo, would be greater than the mask potential, Φe, the mask has greater area. Therefore, only the proper ratio of Φo to Φe will allow the ions to pass through the collecting orifice for a given set of free stream and boundary conditions. The electron motion in this case cannot be ignored, and the equilibrium assumption for the electrons is no longer valid. This is the major complication introduced by the negative ion collection which was not encountered in the sampling of positive ions.

These complications can be seen by comparing the electron and ion velocities. The thermal velocities for the electrons and ions are given by

$$\bar{V}_i = \sqrt{2\frac{k}{m_i}T_i} \qquad \text{for ions}$$

$$\bar{V}_e = \sqrt{2\frac{k}{m_e}T_e} \qquad \text{for electrons}$$

where T_i, T_e = ion and electron temperatures

m_i, m_e = ion and electron masses

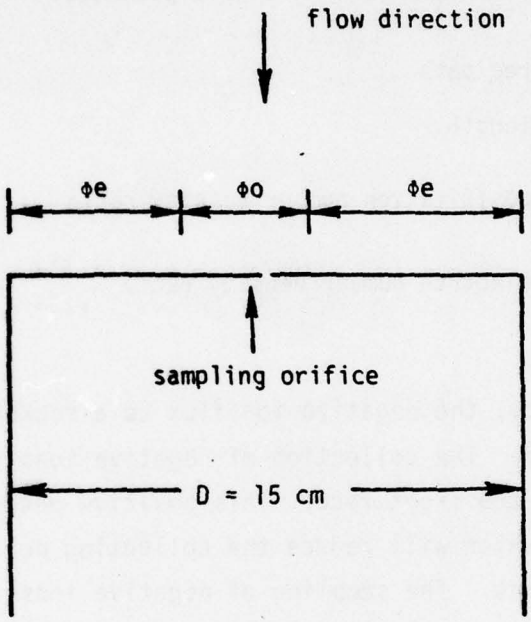

Φo = positive collection potential for negative ion

Φe = negative electron mask potential

Figure 1. Front Face Geometry

The ratio of these speeds are given by

$$\frac{\overline{V}_e}{\overline{V}_i} \simeq \sqrt{\frac{m_i}{m_e}} \sqrt{\frac{T_e}{T_i}}$$

which for equal temperatures, $T_i = T_e$, and an ion molecular weight of 30 becomes

$$\frac{\overline{V}_e}{\overline{V}_i} = 235$$

Since the vehicle or free stream velocity, U_∞, is roughly 3 to 5 times the ion thermal speed, the ions are characterized by the free stream velocity

$$U_i \simeq U_\infty \simeq 4\,\bar{V}_i$$

whereas the typical electron velocity is the thermal velocity

$$U_e \simeq V_e \simeq 235\,V_i \simeq 60\,U_\infty$$

Therefore, for a given time increment, the electron travels a distance 60 times the ion displacement. If the time step in the Monte Carlo calculations is given by Δt_i for the ions, the result requires 60 electron time steps to equal Δt_i. In other words, each ion calculation requires 60 electron calculations. This number can be reduced by recalling that both the electrons and ions are trace species and that encounters between charged particles are neglected except through their coupling in the electric potential. The only direct interactions are collisions between the charged particles and the neutral molecules which can be characterized by the mean free paths

$$\lambda_{en} = \frac{1}{\sqrt{2}\,Q_{en}\,N_n} \qquad \text{for electrons/neutrals}$$

$$\lambda_{in} = \frac{1}{\sqrt{2}\,Q_{in}\,N_n} \qquad \text{for ions/neutrals}$$

where N_n = number density of neutrals

Q_{en}, Q_{in} = collision cross sections

Assuming hard spheres, the collision cross sections for two different particles is given by

$$Q_{12} = \pi \left(\frac{\sigma_1 + \sigma_2}{2} \right)^2$$

where σ_1, σ_2 = particle diameters

For the ions, $\sigma_i \simeq \sigma_n$ and $Q_{in} \simeq \pi \sigma_n^2$, but for the electrons $\sigma_e << \sigma_n$ and $Q_{en} \simeq \pi \frac{\sigma_n^2}{4}$. The ratio of mean free paths is then given by

$$\frac{\lambda_{en}}{\lambda_{in}} = \frac{Q_{in}}{Q_{en}} \simeq 4$$

Therefore, if an ion travels a distance λ_{in} in time increment Δt_i an electron displacement can be $\lambda_{en} \sim 4\ \lambda_{in}$. This reduces the number of electron time steps to equal Δt_i from 60 to 60/4 = 15. In rough terms, this means that the negative ion collection calculations will take approximately 15 times as long as the equivalent positive ion calculation which ignored the electron trajectories.

The procedure to be used in the negative ion sampling and a number of ways to reduce the computing time is discussed in the next section.

2.2 COMPUTATIONAL PROCEDURES

The calculation procedure for the collection of negative ions is shown in the flowchart on Figure 2. The calculation is split into two parts to reduce the computer time requirements by eliminating unnecessary repetition and proceeds in the following steps:

(1) Initialize the problem by specifying the geometry and flow conditions, e.g.,

- Vehicle velocity
- Mean free path for neutral molecules
- Debye length
- Electric potential distribution on the vehicle.

(2) Since the ions and electrons are trace species, the neutral molecule flowfield can be determined without considering the ions and electrons. The neutral flowfield computed by the Monte Carlo direct simulation method is used as a scattering field for the ion and electron distributions. This calculation is performed only once for a given mean free path and can be used for all Debye lengths. In the collisionless limit, this calculation is bypassed.

(3) The electric potential is, in general, determined from the Poisson equation given by

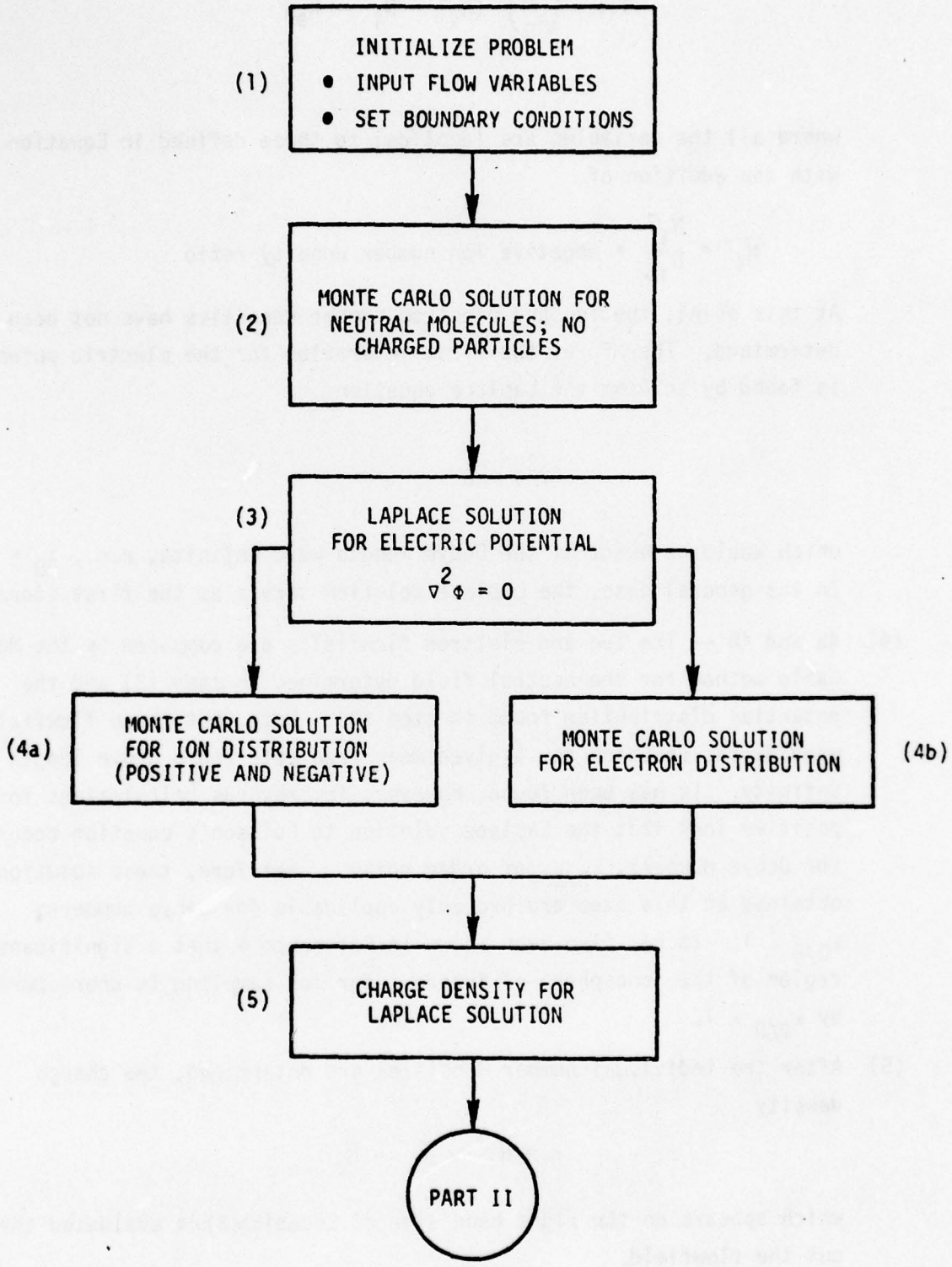

Figure 2. Flow Chart for Part I of Computational Procedure for Negative Ion Collection

$$\nabla^2\phi = \left(\frac{\lambda_\infty}{\lambda_D}\right)^2 (\bar{N}_i^+ - \bar{N}_i^- - \bar{N}_e) \tag{3}$$

where all the variables are identical to those defined in Equation (2) with the addition of

$$\bar{N}_i^- = \frac{N_i^-}{N_{i\infty}} = \text{negative ion number density ratio}$$

At this point, the ion and electron number densities have not been determined. Therefore, the first interation for the electric potential is found by solving the Laplace equation

$$\nabla^2\phi = 0 \tag{4}$$

which would be exact if the Debye length were infinite, e.g., $\lambda_D = \infty$. In the general case, the Laplace solution serves as the first iteration.

(4) 4a and 4b -- The ion and electron flowfields are computed by the Monte Carlo method for the neutral field determined in step (2) and the potential distribution found in step (3). Note that these flowfields provide the solution for a given mean free path and a Debye length of infinity. It has been found, however, in previous calculations for positive ions that the Laplace solution to Poisson's equation occurs for Debye numbers, $\lambda_{D/D}$, of order unity. Therefore, these solutions obtained at this step are probably applicable for Debye numbers, $\lambda_{D/D} > 1$. It has also been shown in Reference 4 that a significant region of the ionosphere of interest for ion sampling is characterized by $\lambda_{D/D} > 1$.

(5) After the individual number densities are determined, the charge density

$$\rho = \bar{N}_i^+ - \bar{N}_i^- - \bar{N}_e$$

which appears on the right hand side of Equation (3) is evaluated throughout the flowfield.

The calculations from (1) through (5) are not repeated in the calculation for a given set of flow parameters and are separated for subsequent calculations and designated as Part I. This division is also made since steps (1) through (5)

are performed for a Debye length of $\lambda_D = \infty$ which must be repeated in principle for every calculation where all the parameters are constant except the Debye length. Therefore, to eliminate repetition of a time consuming procedure, the information generated in Part I, e.g.,

(1) Boundary and initial conditions

(2) Neutral molecule flowfield

(3) Laplace solution

(4a) Ion flowfield

(4b) Electron flowfield

(5) Charge density

will be stored on a parmanent file and recalled and used for calculations involving different Debye lengths for the same values of the other parameters.

Part II.a which is dependent on the Debye length is shown in Figure 3 and begins with step (6).

(6) A solution to Poisson's equation for the charge density distribution computed in step (5) and the proper Debye length, λ_D.

The following steps describe the basic iteration procedure to determine the electron and ion flowfields consistent with the Poisson equation and the neutral molecule distribution from step (1). Since this is a new computation procedure, the optimum method to perform these calculations has not been determined. Therefore, two methods, Part II.a and Part II.b were developed and compared. Note that in either case the ion and electron motions are coupled only through the electric potential since both are trace species and only encounters with the neutral background molecules are important. The first method is shown in Figure 3 in steps (7) through (10).

(7) Electron movement -- The ions and neutrals are assumed stationary in this step and the electron motion is computed for the current electric potential distribution. As discussed in the previous section, the higher speeds associated with the electrons requires that approximately 60 time steps are required for the electrons for each ion time step. However, the difference in the man free paths reduces this ratio from 60 to 15. Therefore, for a fixed movement time interval, Δt_m, the electrons require 15 more calculations than for the ions.

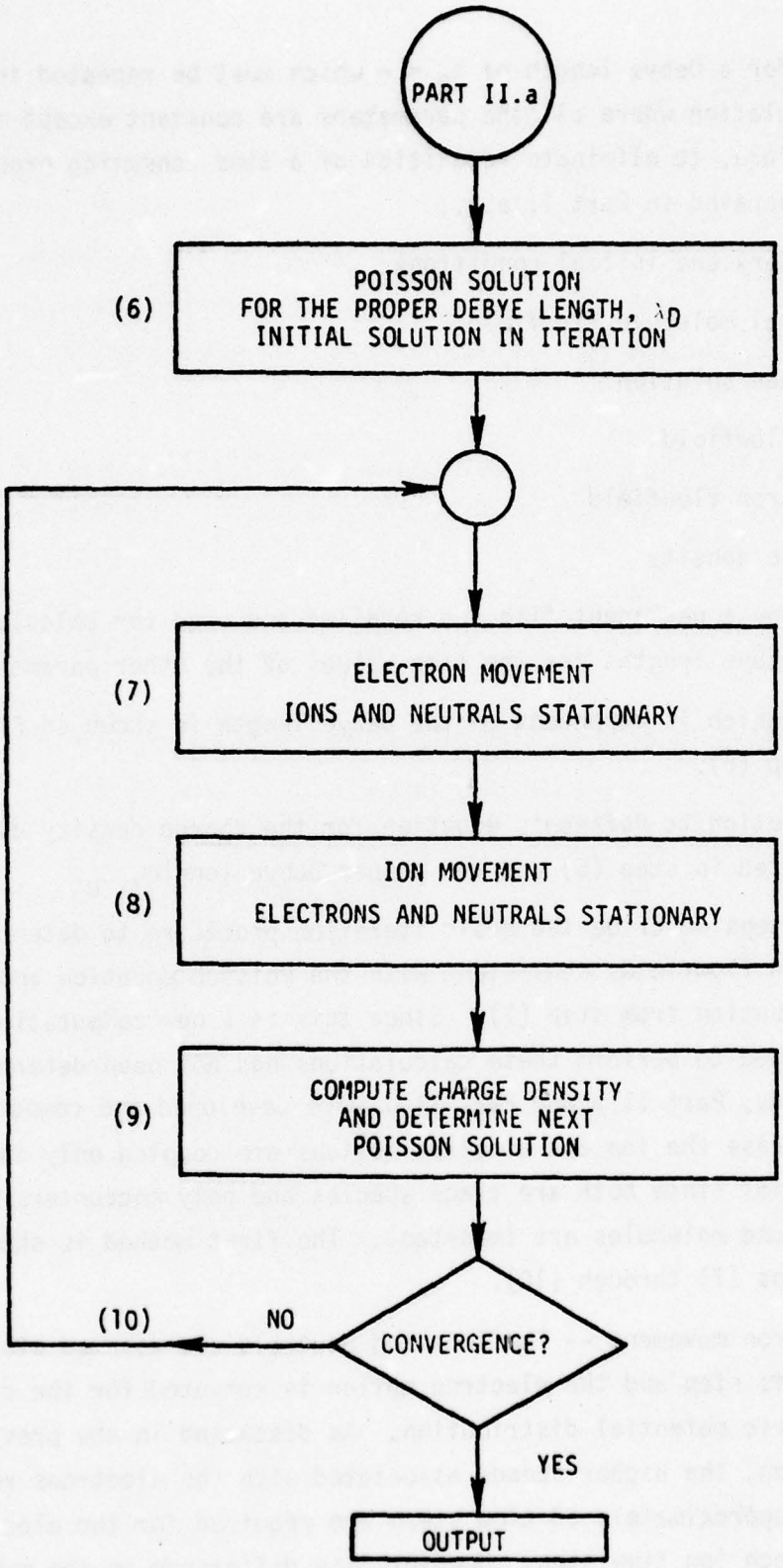

Figure 3. Flow Chart for Part II.a; Iteration Procedure for Negative Ion Collection

(8) Ion movement -- The electrons and neutrals are kept stationary and the ion motion, both positive and negative, is computed for the current electric potential. Note that the electric potential has not been updated between (7) and (8), but the influence of recalculating the potential after step (7) will be investigated.

(9) Electric potential -- The new charge density and electric potential will be computed for the electron and ion distribution calculated in steps (7) and (8).

(10) Convergence test -- Convergence of the electron and ion distributions for a consistent Poisson solution and the neutral molecule distribution will be assessed in step (10). This will be accomplished by checking the charged particle distributions for the current results with the previous iteration. If the comparisons are satisfactory, the results are printed; if not, the iteration continues by returning to step (7).

The alternate procedure to determine the electron and ion distributions, labeled Part II.b, is shown in Figure 4. In both Part II.a and II.b, the initial calculations performed in steps (1) through (6) are identical and only the iteration procedure is changed. Part II.b has three iteration loops compared to one for Part II.a and is described below.

(7) Electron movement and iteration -- The ion and neutral distributions are fixed and the electron flowfield is determined. This calculation differs from Part II.a in that the "steady state" electron distribution is determined for a Poisson solution consistent with the electron motion and the stationary ion and neutral fields. Since only the electrons are in motion, the time steps are independent of the ion time steps and are not constrained as in step (7) of Part II.a.

(8) Ion movement and iteration -- Using the electron density and the potential found in step (7), the positive and negative ion trajectories are determined. Again, the neutral molecules are fixed and the Poisson solution, consistent with the ion motion, is determined.

(9) Convergence test -- The electric potential distributions computed in (7) and (8) are compared for convergence. If the potentials are acceptably similar, the results are printed; if not, the iteration returns to step (7).

At the start of the present study no direct comparisons were available between the procedures and potential advantages are apparent in both. For example, in

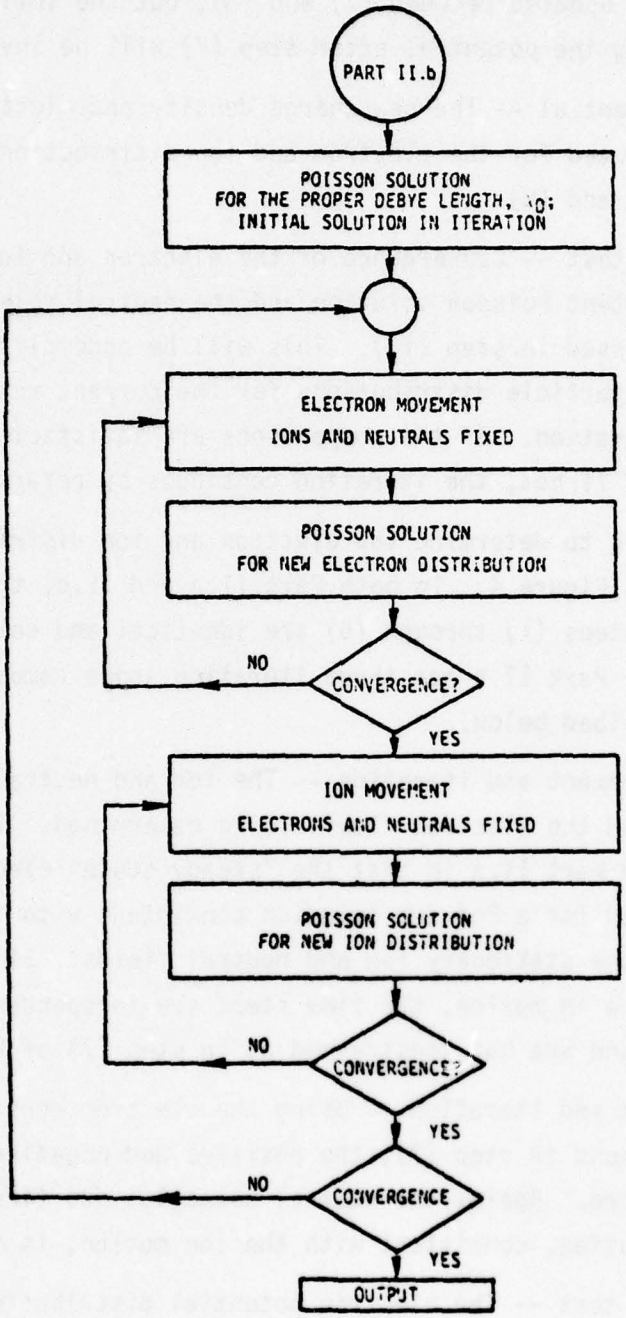

Figure 4. Flow Chart for Part II.b; Iteration Procedure for Negative Ion Collection

II.b there is no constraint on the time step for the movement of the electrons as in II.a. Therefore, the electron iterations should be as fast as the ion iterations, but the convergence between the ion and electron fields could eliminate any potential advantage over II.a. In the method proposed in II.a, the electron iteration was estimated to be 15 times greater than the ion calculation for a given time interval. Therefore, this method is not feasible unless the electron time step can be increased in practice. For example, if a typical ion convergence without electrons takes 10 minutes on the CDC 6600, the electron calculations would take 150 minutes which is clearly unacceptable (for low altitude results involving many collisions, this number could be doubled). An upper limit on the entire calculation of approximately 60 minutes requires that the time factor be reduced from 15 to 5. Another computational method which would accelerate the calculations would be to make better use of weighting factors for the charged particles so that the number of particles in the calculation could be reduced. No attempt to implement these efficiencies was made in the previous calculations since the computation times for the positive ion collection were well within reasonable constraints. Both methods have been implemented and a few test cases have been computed. From these preliminary results the method designated as II.b appears to converge faster. No conclusions were made during the reporting period due to the observation that the electron effects were not simulated properly. This is discussed in the next section.

2.3 CHARGED PARTICLE-NEUTRAL INTERACTION

Monte Carlo calculations performed for the electron motion in a neutral gas at densities where collisions are important indicated that the drift velocities were too high. After confirming the correctness of the numerical procedure, the basic assumptions for the simulation were reexamined.

In the past simple hard spheres were used for the charged particle-neutral scattering model and the collision cross section was computed from

$$Q_{pn} = \pi\left(\frac{\sigma_p + \sigma_n}{2}\right)^2$$

where σ_p = charged particle diameter

σ_n = neutral particle diameter

For the ions (p = i)

$$Q_{i_n} = \pi\left(\frac{\sigma_i + \sigma_n}{2}\right)^2 \simeq \pi\sigma_n^2 \quad (\sigma_i \simeq \sigma_n)$$

and for the electrons (p = e)

$$Q_{en} = \pi\left(\frac{\sigma_e + \sigma_n}{2}\right)^2 \simeq \pi\frac{\sigma_n^2}{4} \quad (\sigma_e << \sigma_n)$$

The simple hand sphere model used for convenience in the earlier studies was justified on the basis that the gross features of the ion collection process were not clearly understood and in the collection of positive ions the electron trajectories were not computed. However, the present task of simulating the collection of negative ions requires accurate calculations of the electron motion.

The proper description of the charged particle-neutral encounter can be represented by an interaction potential of the form

$$V(r) = Ae^{-\beta r} + \sum_{n=4} C_n r^{-n}$$

where the first term represents strong, short range repulsive forces due to ordinary neutral particle gas kinetics and the succeeding terms represent attractive forces which arise between the charged particle and the polarized structure of the neutral.

In the calculations presented here a 4^{th} power attraction suggested originally by Langevin was used. The attractive force, due to polarization of the neutral molecule is given by

$$F = \frac{2\mu e^2}{r^5}$$

where μ = polarizability

e = electronic charge

The current Monte Carlo calculations treat the charged particle-neutral encounter as a binary collision involving both attractive and repulsive forces. The particle trajectories due to the repulsive force can be separated into two effects: (1) isotropic scattering at an impact parameter inversely proportional to the relative velocity of the collision, (2) isotropic scattering by a hard sphere core of fixed radius. The dominance of (1), (2) or the attractive force depends on the value of the impact parameter. For low energy encounters the attractive force would dominate, whereas for high energy encounters strong repulsive forces would be most important (see Figure 5).

The collision diameter σ_o for the attractive force is found to be

$$\sigma_o = 2r_o = 2\left(\frac{4e^2\mu}{m^* u_r^2}\right)^{1/4}$$

where $m^* = \dfrac{m_p m_n}{m_p + m_n}$

u_r = relative velocity of the encounter

This diameter can be compared to the standard hard sphere diameter σ_n to illustrate the polarization effect. For example, oxygen has a polarizability

$$\mu \cong 1.6 \times 10^{-24} \text{ cm}^3$$

and a hard sphere diameter

$$\sigma_n \cong 3 \times 10^{-8} \text{ cm}$$

The reduced mass for the ion-neutral interaction becomes

$$m^* = \frac{m_n m_i}{m_i + m_n} \cong \frac{m_n}{2} \quad (m_i \cong m_n)$$

At 300°K the relative velocity can be approximated by

$$u_r^2 \cong \frac{2kT}{m} = 1.4 \times 10^9 \ \frac{\text{cm}^2}{\text{s}^2}$$

Finally the ratio of the diameters is found to be

$$\frac{\sigma_o}{\sigma_n} \cong 5.3$$

This result implies that the collision cross section for oxygen ion-neutral encounters at 300°K is approximately 25 times the typical hard sphere value.

To investigate the results of this collision model a simple relaxation process has been studied. Consider a weakly ionized gas composed of electrons, positive ions and neutral particles which are initially in equilibrium at a single temperature. The positive ions are singly charged and of mass equal to the neutral particles. A prescribed constant electric field is instantaneously applied and subsequently maintained and the molecular motion of the gas is computed in time as a steady state is approached. The physical situation to which this corresponds could be imagined to consist of a gas contained between parallel electrodes of unlimited extent and great separation. Attention is focused upon a thin slab of this gas within which the spatial gradients can be ignored. Since all charged-charged interactions are contained in the electric field, which is known and constant for this case, the electron and ion motions are independent. Only the encounters of the charged particles with the neutral particles while under the influence of the electric field determine the behavior of the charged particles.

Quantities of interest for this study are the following:

1) the steady state drift velocity per unit field, e.g. the mobility
2) the relaxation times
3) the temperature and shape of the distribution function in the steady state

In the ion collection process by a rocket borne mass spectrometer biased at a potential ϕ the parameter $e\phi/kT$ is used to characterize the strength of the electric field. In the present example of a gas contained between parallel electrodes the parameter E/P, field strength over neutral gas pressure, is used. The acceleration of a particle with charge e and mass m in an electric field E is eE/m. The energy acquired by the particle from the field between collisions is approximately $eE\cdot\lambda$ where λ is the mean free path. Since λ is inversely proportional to the density

$$E \cdot \lambda \sim E \cdot \frac{1}{P} \sim \frac{E}{P} \cdot T$$

or

$$\frac{E\lambda}{T} \sim \frac{E}{P}$$

Therefore the ratio of the field energy to thermal energy is proportional to E/P. This result assumes the field strength is low and that the masses of the ion and neutral particle do not differ greatly (thus excluding electrons). For arbitrary field strength and ion mass, E/P is less useful. However, most experimental data are presented in terms of it.

Results of computations made with this model is shown in Figures 6 through 9. Here the product of the mobility

$$K = \frac{V_d}{E}$$

where V_d = drift velocity

E = electric field

and the pressure, p, in atm is shown for the electrons in a neutral gas with molecular weight 29. The calculations compare adequately with the experiments which have been influenced by effects not modeled in the simulation such as charge transfer, quantum mechanical resonance effects and clustering.

2.4 NEGATIVE ION COLLECTION - COLLISIONLESS RESULTS

A series of calculations have been performed to predict the collection of negative ions to the probe geometry shown in Figure 1. The ratio of the positive collection potential to the negative electron mask potential, $\gamma = \Phi_o/\Phi_e$, was fixed at -10 and the ratio of the disk radii, $\alpha = r_o/r_e$, was varied. The critical value of γ is given by[5]

$$-\gamma_c = \frac{\sqrt{1-\alpha^2}}{1-\sqrt{1-\alpha^2}}$$

For values of $|\gamma| < |\gamma_c$ a repelling potential exists along the centerline which retards the collection of the negative ions. This function is shown in Figure 10 and indicates that for $\gamma = -10$ a repelling potential will exist for $\alpha < 0.4$.

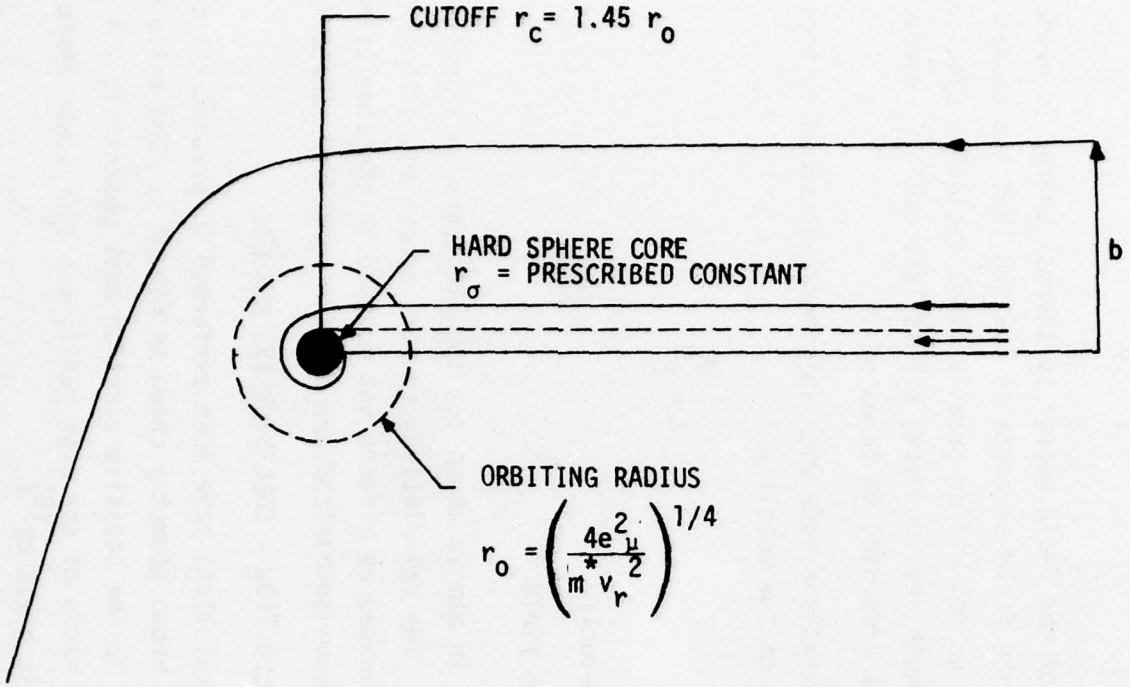

Figure 5. Charged-Neutral Scattering Model

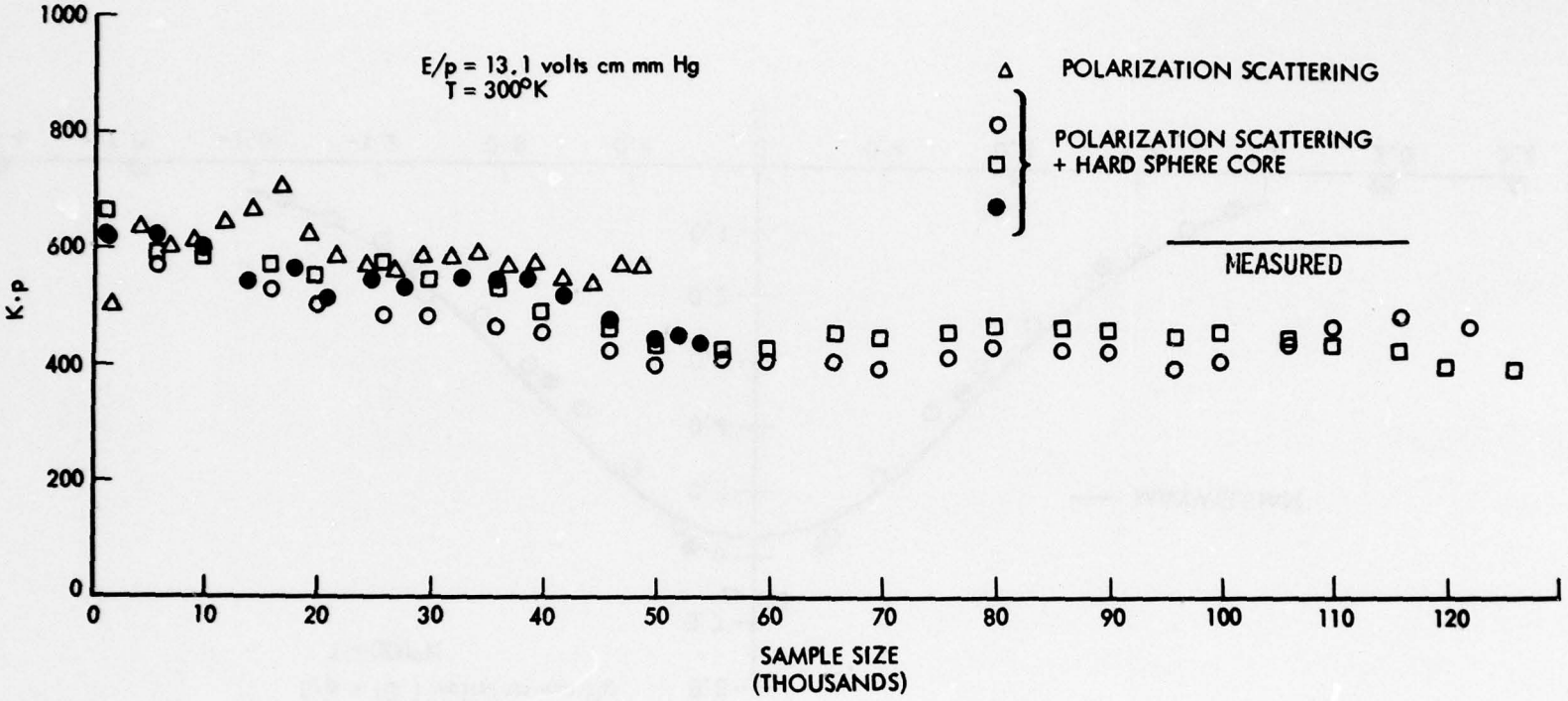

Figure 6. Electron Mobility

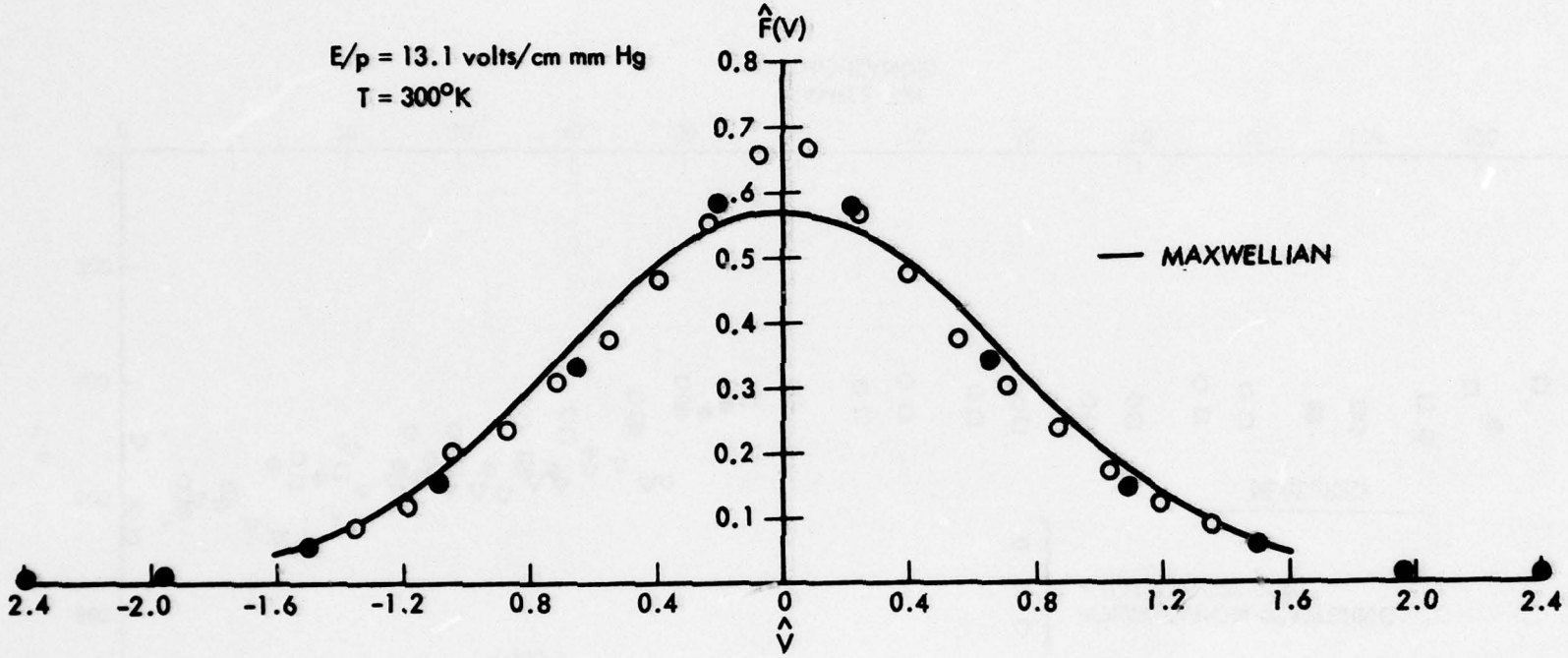

Figure 7. Electron Velocity Distribution

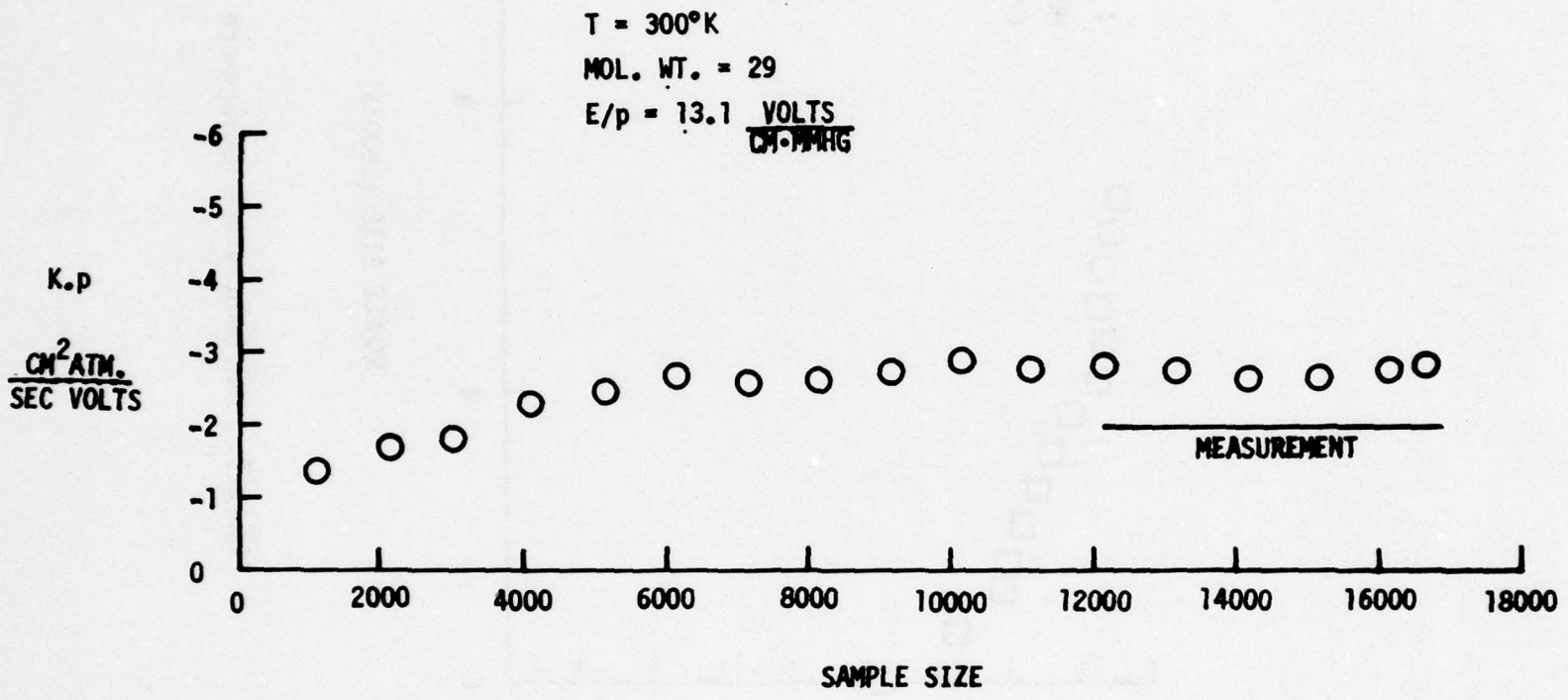

Figure 8. Ion Mobility

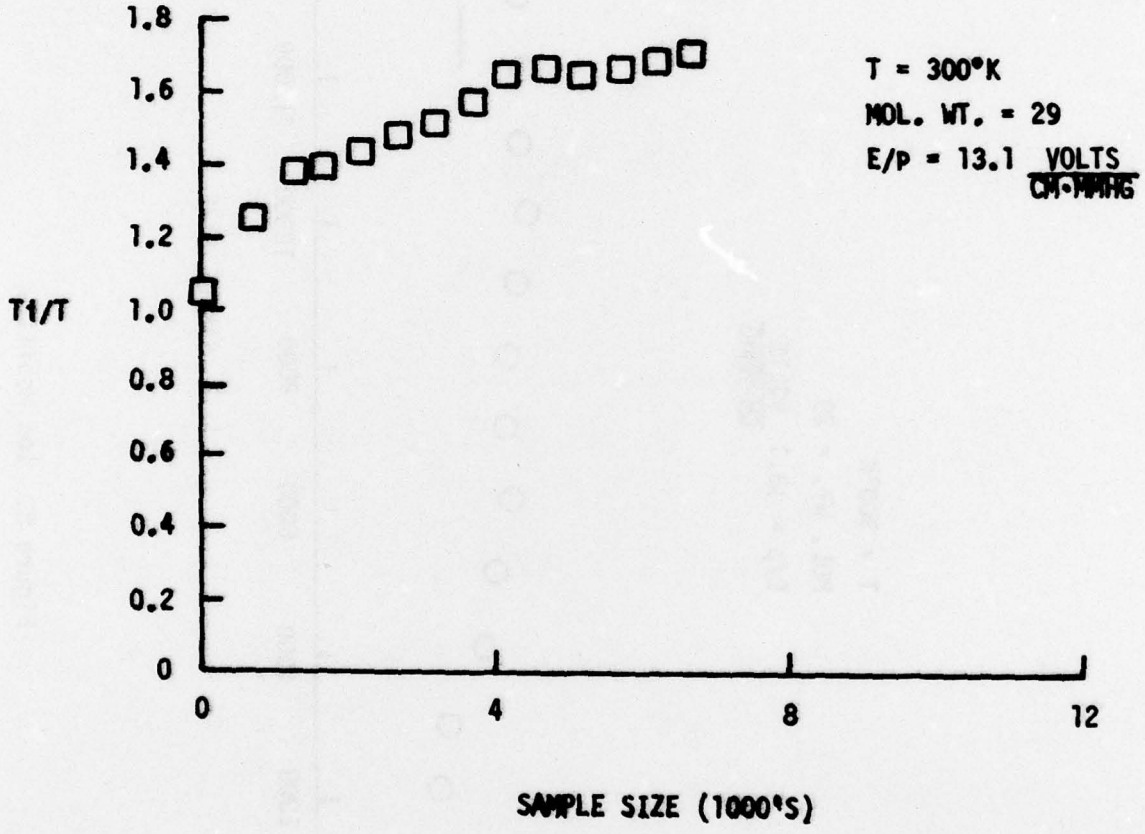

Figure 9. Ion Temperature Convergence

Figure 11 shows the variations of the centerline potential for the following conditions,

Speed ratio $s = 3.10$ $\quad \Phi_o = 200$ $\quad \Phi_e = -20$

Knudsen number $\frac{\lambda_\infty}{D} = 1000$

Debye number $\frac{\lambda_D}{D} = 1000$

and α from 0.08 to 0.75. The potentials for $\alpha = 0.08$ and 0.25 exhibit the change in sign of potential as expected and the result for $\alpha = 0.42$ appears to be at the transition point. For the largest value of $\alpha = 0.75$ the potential decays in a monotonic way. The flux of positive ions collected by the probe point is shown in Figure 12 as a function of the collecting radius. For $\alpha = 0.08$ which resulted in a maximum repelling potential of approximately $\phi \tilde{=} -7$ there is no flux of negative ions to the front face. However, for $\alpha = 0.25$ with a small repelling potential of $\Phi \tilde{=} -1$ the kinetic energy of the negative ions was sufficiently higher than the retarding electric field to establish a flux coefficient at the stagnation point of approximately $C_I = 10$. As the value of α is increased, the flux coefficient changes only slightly as α varies from 0.58 to 0.79.

Although these calculations were performed for a Debye number large enough to neglect the charge density effects, the electron flow field and flux to the front face must be computed to determine the current.

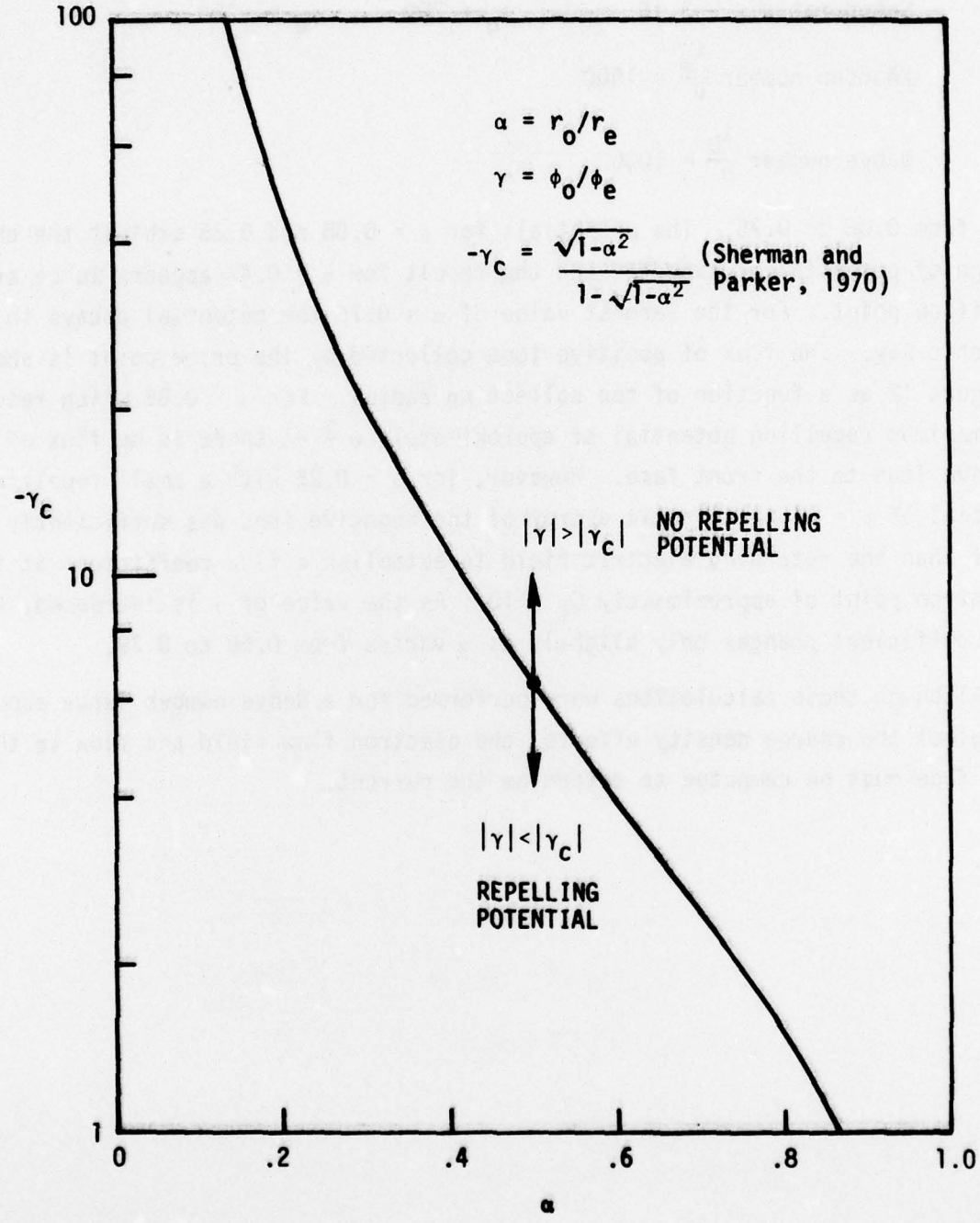

Figure 10. Critical Potential Ratio

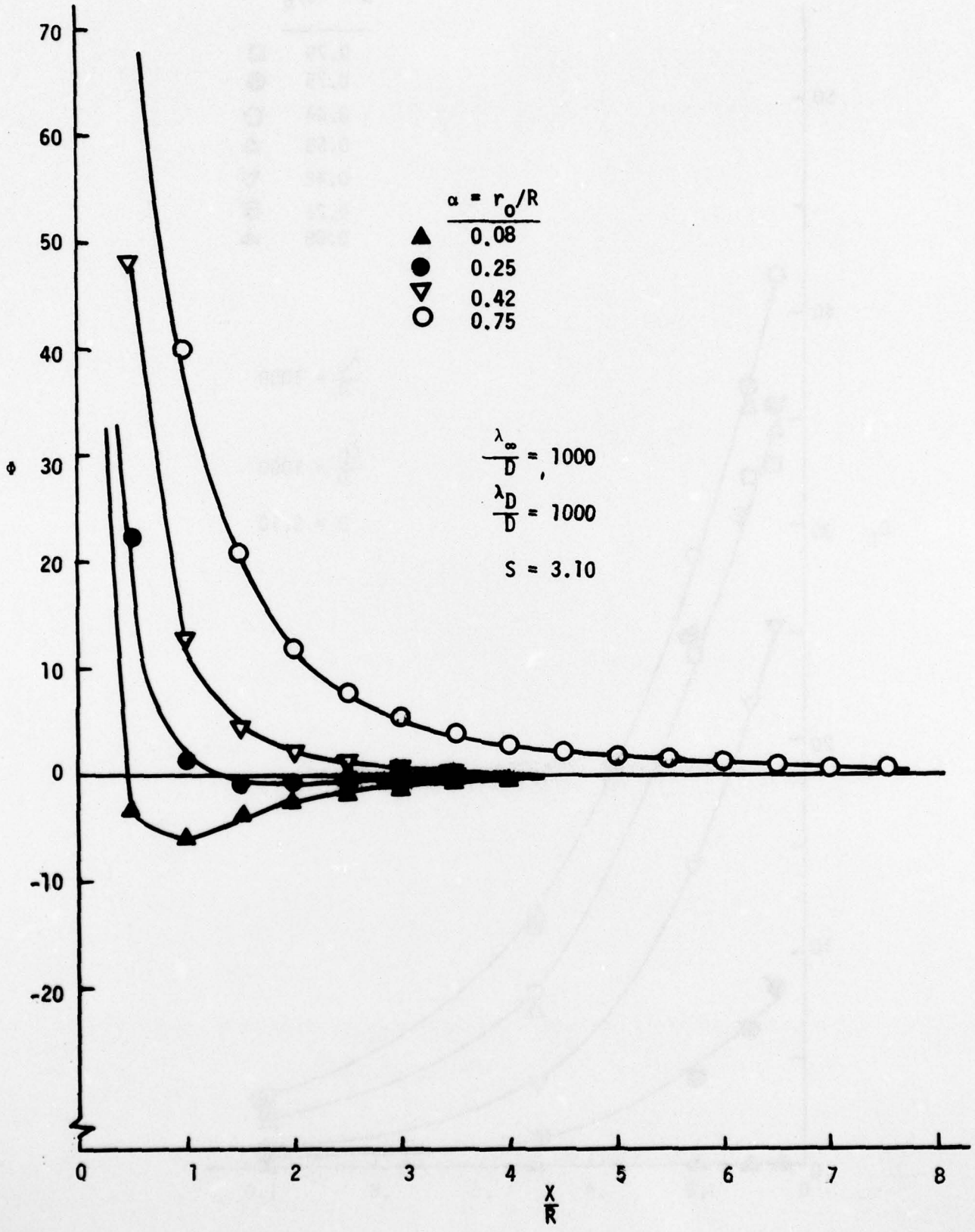
70
60
50
40
30
20
10
0
-10
-20
Φ
α = r_o/R
0.08
0.25
0.42
0.75
λ∞/D = 1000
λD/D = 1000
S = 3.10
0
1
2
3
4
5
6
7
8
X/R

Figure 11

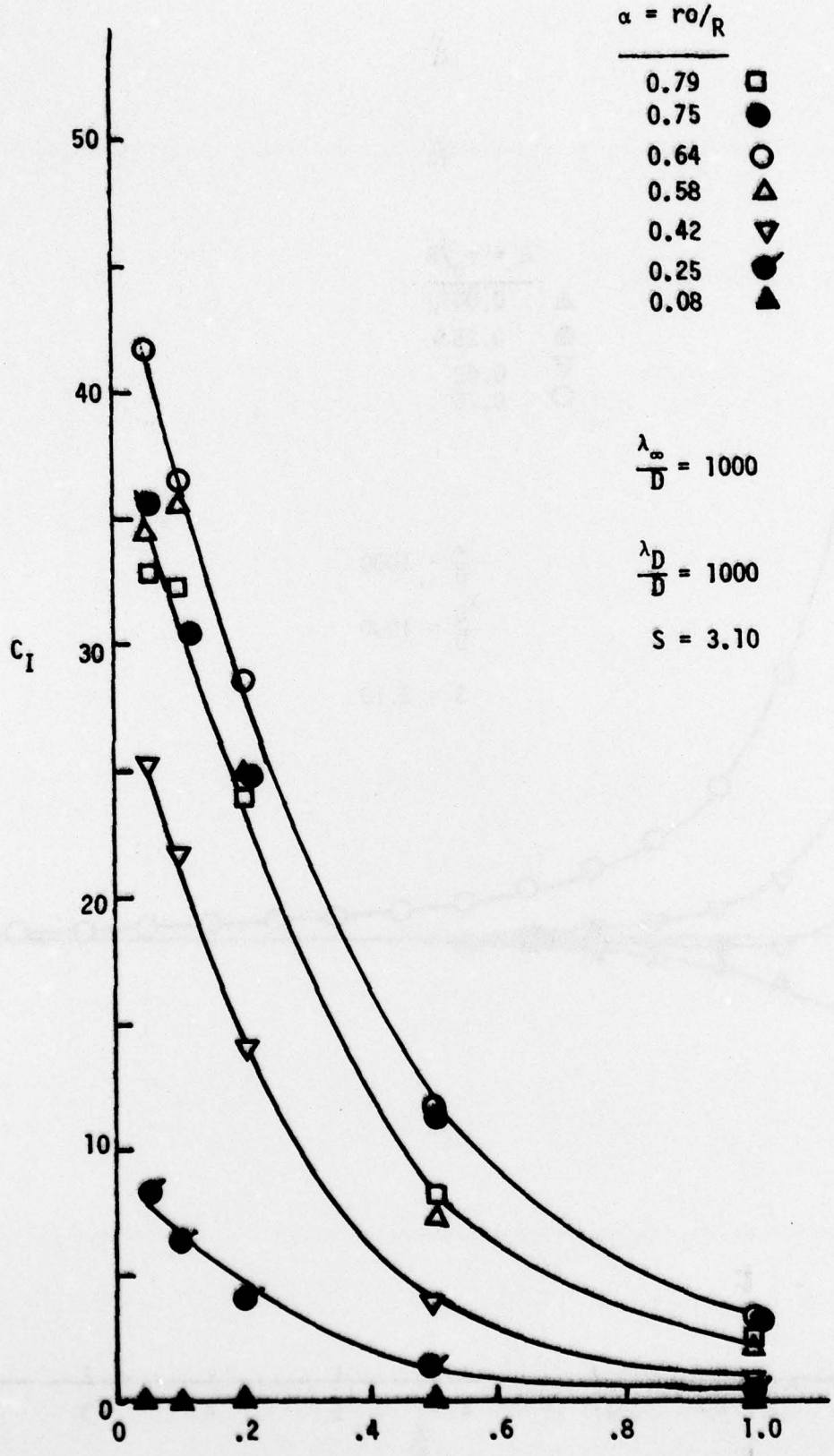
α = ro/R
0.79
0.75
0.64
0.58
0.42
0.25
0.08
λ∞/D = 1000
λD/D = 1000
S = 3.10
C_I
50
40
30
20
10
0
0
.2
.4
.6
.8
1.0

Figure 12

3. CONCLUSIONS

The efforts to extend the Monte Carlo Method to the collection of negative ions have been shown to be more difficult than anticipated. It was found that the electron trajectories must be determined carefully and that the effect of polarization are important in electron-neutral collisions. In addition, the Monte Carlo computer code which was developed for the negative ion collection stretched the computer resources of the CDC6600. Future efforts will include the implementation of more efficient programming techniques to reduce the core requirements and computation times.

REFERENCES

1. Vogenitz, F. W., "Computer Simulation of Ion Collection by an Ionospheric Probe," TR-0006, Air Force Cambridge Research Lab., Bedford, Massachusetts, January 1973.

2. Sugimura, T. and Vogenitz, F. W., "Monte Carlo Simulation of Ion Collection by a Rocket Borne Mass Spectrometer for Collisionless and Transitional Flowfields," TR-73-0448, Air Force Cambridge Research Lab., Bedford, Massachusetts, July 1973.

3. Sugimura, T. and Vogenitz, F. W., "Monte Carlo Simulation of Ion Collection by a Rocket Borne Mass Spectrometer," Journal Geophysical Research, Vol. 80, No. 4, February 1975.

4. Sugimura, T., "Prediction of Positive Ion Collection by a Rocket Borne Mass Spectrometer," presented at 10th International Symposium on Rarefied Gas Dynamics, Aspen, Colorado, Paper No. 59, July 19-23, 1976 (to be published in the proceedings).

5. Sherman, C. and Parker, L. W., "Potential Due to a Circular Double Disk," AFCRL-70-0568, Air Force Cambridge Research Lab., Bedford, Massachusetts, 12 October 1970 (also Journal of Applied Physics, Vol. 42, No. 2, February 1971).